

Interface Sensitized Optical Microfiber Biosensors

Bai-Ou Guan , Member, IEEE, and Yunyun Huang 

(Invited Paper)

Abstract—Sensitivity is an important parameter to characterize the performance of sensors. Interfacial modification and functionalization is an effective strategy to improve the sensitivity of optical biosensors. This paper reports our recent development on interface sensitized fiber optic biosensors for the detection of ultra-low concentration of biological targets. We employ microfiber mode interferometer as transducer to sense the molecular binding interaction induced surrounding refractive index change. By modifying the microfiber surface to increase the assembling surface area and enhance the evanescent field energy density, ultra-low limit of detection of 1.65×10^{-15} M and 6.82×10^{-17} M, respectively, were realized for neurotransmitter γ -amino-butyric acid and cellular cytochrome c.

Index Terms—Biosensors, evanescent wave, interfacial sensitization, optical microfiber.

I. INTRODUCTION

IN NUMEROUS fields such as medical diagnosis, environmental monitoring, or quality control in the food industry, the rapid and accurate detection of analytes (proteins, DNA, pathological markers, toxin etc.) in small concentration is crucial [1]. Fiber optic biosensors are powerful detection and analysis tools, which are small in size, light in weight, immune to electromagnetic interference, capable of distributed sensing and remote sensing. They are suitable for the in-situ or in-vivo application to detect and measure chemical and biological parameters, such as pH value, ions, and biological molecules [2]. Optical fibers are inherently insensitive to biological analytes. The detection of biological targets is achieved by biorecognition elements which are immobilized onto the fiber surface. The biorecognition elements can distinguish the target molecules from the environment and specifically capture the targets. The binding interaction of the biorecognition elements with the target molecules induces a measurable change of optical signal. According to the working principle, fiber optic biosensors can be divided into two categories: refractive index (RI) based fiber optic biosensors and fluorescence-based fiber optic biosensors. The RI-based biosen-

sors detect the RI change near the fiber surface induced by the molecular binding interaction through the evanescent field of the fiber [3]. For fluorescence-based biosensors, the recognition molecules or target molecules are labeled with fluorophores, and the molecular binding interaction causes a change in the intensity, wavelength, polarization state, or lifetime of the fluorescent signal [4]. A difference is that, in fluorescence-based biosensors, the fiber only acts to deliver the excitation light and fluorescent signals, whereas in RI based biosensors, the fiber participates in the transduction process and therefore provides the ability to enhance the sensor response through flexible and diverse fiber optic RI transducer design.

Sensitivity is an important parameter to characterize the sensor performance. Sensitivity refers to the output produced by a sensor from a unit input under static conditions. The output signals of different sensors can be in various forms such as wavelength, intensity, or phase. Because the output signals are different in form, the sensitivity magnitude of different sensors is not comparable. Limit of detection (LOD), which refers to the minimum detected concentration that the sensor can distinguish from noise, is another important parameter that evaluates sensor performance and provides comparability between different sensors. Obviously, LOD is strongly dependent on the sensitivity and can be improved by enhancing the sensitivity. Although fluorescence-based biosensor and RI based biosensor have the above differences, the sensitivity of both can be improved through some of the same strategies, for example, by catalyzing or cascade reaction to amplify the molecular binding interaction induced effects [5]–[8]. The biosensors operate in a liquid environment and thus forms a solid-liquid interface on the sensor surface where molecular binding and light-matter interaction occur. The interfacial modification and functionalization are effective strategies to improve the sensitivity [9]–[12]. Specifically, the sensitivity can be improved from the two aspects: (1) assembling more biorecognition elements on the fiber surface to form more binding sites and therefore enhancing the ability to capture target molecules; (2) enhancing the energy density of the evanescent field, thereby enhancing the light-matter interaction.

In this paper, we report the progress of our recent development on interface sensitized optical microfiber biosensors. We review our works in modifying the microfiber surface to enlarge the assembling surface area and enhance the evanescent field energy density, and thereby increase the sensor sensitivity. The paper is organized as follows. In Section II, the working principle of microfiber mode interferometer RI transducer is introduced. In

Manuscript received November 2, 2018; accepted November 15, 2018. Date of publication December 24, 2018; date of current version May 1, 2019. This work was supported in part by the National Natural Science Foundation of China under Grant U1701268 and Grant 51773084 and in part by the Fundamental Research Funds for the Central Universities under Grant 21617420. (Corresponding author: Bai-Ou Guan.)

The authors are with the Guangdong Provincial Key Laboratory of Optical Fiber Sensing and Communications, Institute of Photonics Technology, Jinan University, Guangzhou 510632, China (e-mail: tguanbo@jnu.edu.cn; thuangyy6@jnu.edu.cn).

Color versions of one or more of the figures in this paper are available online at <http://ieeexplore.ieee.org>.

Digital Object Identifier 10.1109/JLT.2018.2889324

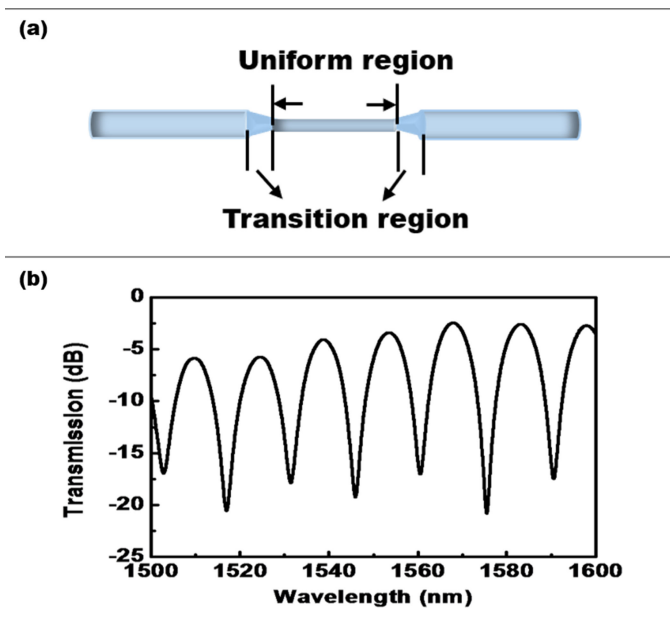


Fig. 1. (a) Schematic diagram of microfiber mode interferometer. (b) Typical transmission spectrum of microfiber mode interferometer.

Section III-IV, microfiber mode interferometer biosensors for the detection of ultra-low concentration of neurotransmitter and cellular cytochrome c are presented, and interfacial sensitization by enlarging the assembling surface area and enhancing the evanescent field energy density are demonstrated. A brief conclusion is given in Section V.

II. FIBER OPTIC RI TRANSDUCER

Compared to fluorescence based biosensors, an advantage of RI based biosensors is that they are more flexible and versatile in implementation, with more powerful design capabilities. Various fiber optic structures have been demonstrated as RI transducers for the implementation of biosensors, such as long-period fiber gratings [13]–[15], microfiber Bragg gratings [16]–[18], tilted fiber Bragg gratings [19]–[21], Fabry-Perot or Mach-Zehnder interferometers [22]–[26]. By optimizing the design, some structures can achieve very high RI sensitivity. The focus of this article is not on the transducer design, but on how to improve sensor sensitivity through interfacial engineering. Here optical microfiber mode interferometer is employed as RI transducer.

Fig. 1 shows the schematic diagram of the microfiber mode interferometer. It is a biconical fiber taper structure, consisting of a diameter decreasing transition region, waist region with a diameter of microns, and a diameter increasing transition region. The fiber is abruptly tapered to the waist diameter. The taper angle is large enough that, at the diameter decreasing transition region, some light energy in the fundamental HE_{11} mode is coupled into the higher order HE_{12} mode. After transmission through the waist region, this part of the light is recombined with the fundamental HE_{11} mode at the diameter increasing transition region, and generates interferometric pattern in the fiber transmission spectrum. Because a fraction of the HE_{12} mode energy spreads out of the fiber cladding to interact with the

surrounding medium, and therefore the interferometric pattern shifts with surrounding RI [27]–[29].

The microfiber mode interferometer can be easily fabricated by heating and stretching a section of normal fiber. By optimizing its design, the RI sensitivity as high as 10^4 of nm/RIU can be achieved. It has the advantages of designable RI sensitivity, ease of production, low cost, and suitable for medical disposable use. In our experiments, the microfiber mode interferometers were fabricated by flame brushing technique. The typical parameters are as follows: waist length of 6–7 mm, waist diameter of 6–8 μm , RI sensitivity of ~ 2500 nm/RIU.

III. INTERFACE SENSITIZED NEUROTRANSMITTER SENSORS

As a major inhibitory neurotransmitter in human brain, γ -amino-butyric acid (GABA) is involved in nearly all brain circuits [30]. Its concentration fluctuation is associated to the formation of some neurological disorders including epilepsy, seizures, convulsions, Huntington’s disease and Parkinsonism [31]. The real-time and in-situ detection of ultra-low concentration GABA molecules is of great significance for revealing the mechanisms of neurological diseases formation and preventing possible neural disorders occurrence. In this section, interface sensitized microfiber biosensors for ultra-low concentration GABA detection based on the assembling surface area enlargement and the evanescent field energy density enhancement will be demonstrated.

A. Enlarging the Assembling Surface Area

As mentioned previously, the detection of biomolecules by the fiber optic sensor is achieved through recognition elements assembled onto the fiber surface, which specifically capture and interact with the target molecules, thereby inducing a change of the surrounding RI. The amount of recognition elements has an impact on the sensitivity. The more recognition elements immobilized onto the fiber surface, the stronger the ability to capture the target molecules, and hence the more sensitive the sensor. For a microfiber mode interferometer, the RI sensitive part is only in the waist region, which is only a few microns in diameter. Since the surface area is relatively small, the amount of recognition elements that can be assembled is very limited. An effective approach to increase the amount of recognition molecules is to increase the assembling surface area of the microfiber waist. By forming more binding sites, the sensor sensitivity can be effectively improved.

To enlarge the assembling surface area, the microfiber surface was functionalized with mesoporous silica microsphere arrays. The surface of the silica microspheres is full of nanopores, which have uniform channels and narrow pore size distribution. The size of nanopore is specially designed to match the target GABA molecules. The nanopores enable the microfiber interferometer to recognize the target molecules by size selectivity. Only the targets with size matching to the nanopores can be captured. Molecules with larger size cannot enter the nanopores. Molecules with smaller size can enter the nanopores and then come out, without staying in the nanopores.

Fig. 2 illustrates the functionalization process of silica microfiber as follow: The silica microfiber was immersed in

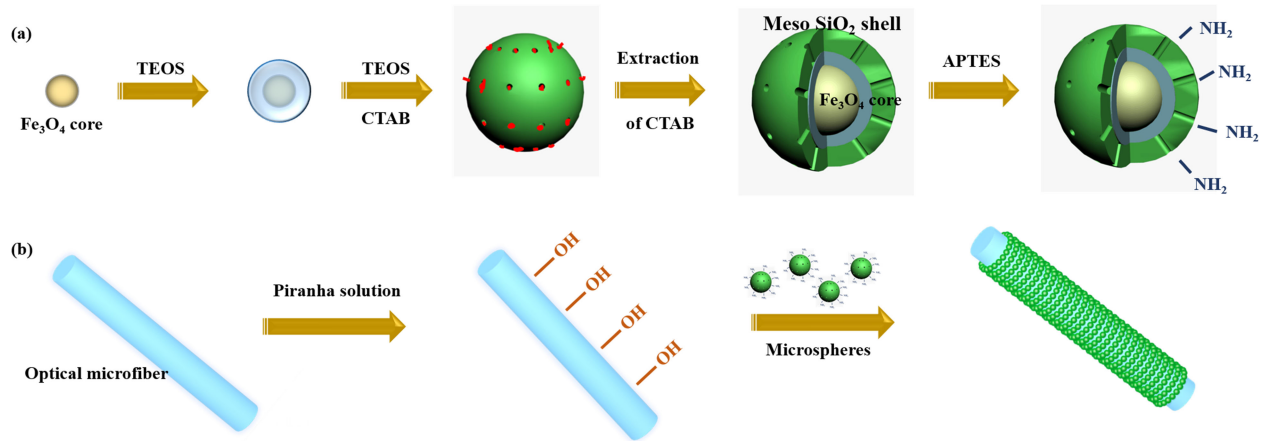


Fig. 2. Schematic of functionalization process of silica tapered optical fiber. (a) Preparation of silica microspheres is full of nanopores. (b) Depositing microspheres on microfiber surface.

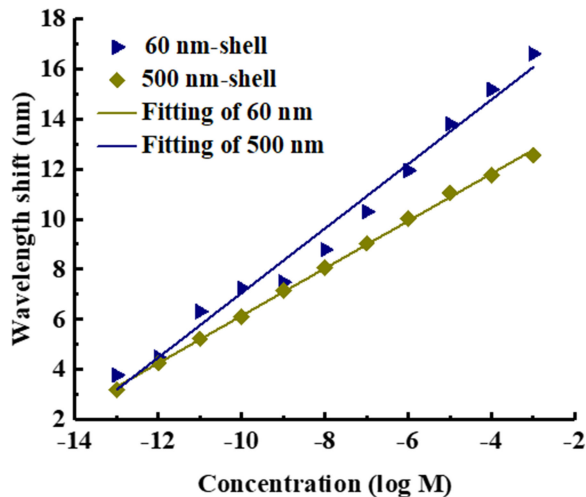


Fig. 3. The dip wavelength versus GABA concentration for the sensors with microspheres size of 60 nm and 500 nm.

piranha solution to produce sufficient reactive hydroxyl groups with negative charge [32]; the microspheres were treated by 3-aminopropyl-triethoxysilane (ATPES) to modify their surface with aminopropyl groups, which were rich of positive charge [33]; finally, the hydroxyl groups on fiber-optic surface and aminopropyl groups on microsphere surface attracted each other by electrostatic attraction and realized the surface functionalization of sensor [34]. Two different sizes of mesoporous microspheres with diameter of 500 nm and 60 nm, respectively, were prepared and assembled onto the microfiber surface. Fig. 3 [34] shows the response of the two sensors with different size of microspheres in GABA solution. The response sensitivity of the sensor with microspheres size of 60 nm and 500 nm is 1.28 nm/log M and 0.94 nm/log M, respectively. The smaller microspheres can provide an improved sensitivity than the larger microspheres. This is because, the microsphere arrays can increase the microfiber surface area, and the smaller the microspheres, the more significant the surface area increasing effect.

In our work, the SiO_2 microspheres improved the LOD to 3.51×10^{-13} M. These high sensitivity, small volume and biocompatibility enable the sensor in precision ultra-diluted GABA detection [34]. Based on a similar strategy to increase the assembling surface area, a microfiber biosensor with nanosphere array possessing nanopores with specified size for the detection of monoamine neurotransmitter, serotonin (5-HT), also presented an improved LOD as low as 84 fM [35]. It shows the interface made up of micro-/nanosphere arrays could enlarge the assembling surface area of the microfiber waist, therefore improve the sensor sensitivity effectively. Furthermore, it is expected that other interfacial structure such as porous membranes [36]–[38] could also enlarge the fiber surface area and thus improve the sensor sensitivity.

B. Enhancing the Evanescent Field Energy Density

The sensing of the RI change by fiber optic transducer is achieved by the interaction of the evanescent field with the surrounding medium. The strength of the evanescent field is a determining factor in sensor sensitivity. Enhancing the evanescent field is also an effective way to improve sensor sensitivity. Reducing the microfiber diameter can increase the proportion of the evanescent field. However, when the proportion of the evanescent field is large to a certain extent, the transmission loss sharply increases as the biosensor works in a liquid environment. An effective strategy is to enhance the energy density of the evanescent field by modifying the microfiber surface. For example, silver nanowires, gold nanocages and nanospheres were modified onto the surface of tilted fiber Bragg grating, and several-fold sensitivity enhancement was realized [39]–[41].

Based on this strategy, we have designed optical microfiber sensors with the near-infrared plasmonic electromagnetic field enhanced interface. Based on the microsphere array functionalized microfiber mentioned above, raspberry-like meso- SiO_2 nanospheres with silver (or gold) nanoparticles covering on silica nanosphere surface with diameter of ~ 150 nm have been developed as shown in Fig. 4 [42]. The construction of nanosphere

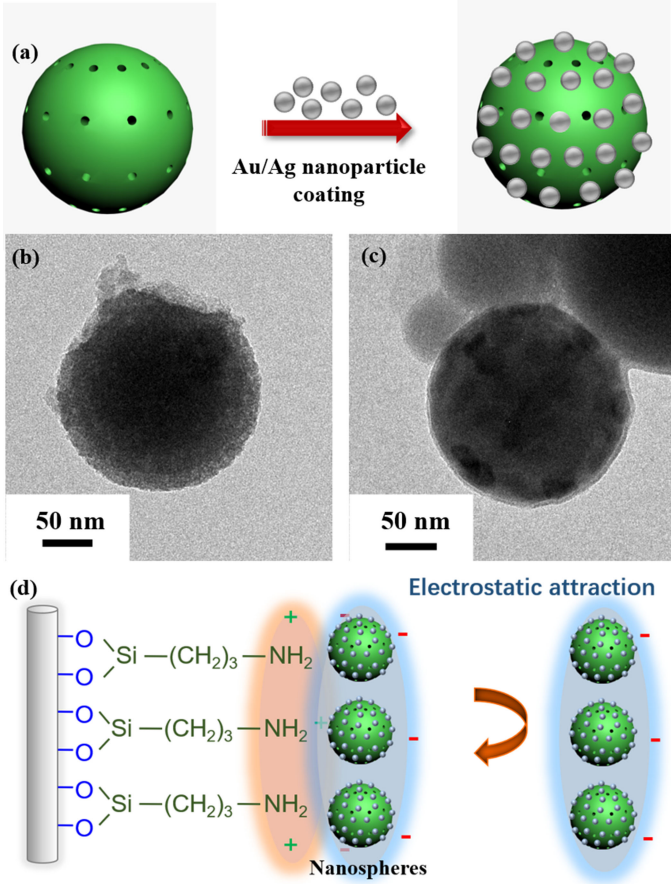


Fig. 4. Schematic of raspberry-like nanosphere-functionalization process on microfiber. (a) Schematic depiction of the fabrication of raspberry-like nanosphere. (b) Transmission electron microscopy (TEM) image of SiO₂ nanosphere before coating of Au/Ag nanoparticles. (c) TEM image of raspberry-like nanosphere after coating of gold nanoparticles with diameter of 10 nm. (d) Schematic of functionalization process of raspberry-like nanospheres onto microfiber surface.

with 150 nm-diameter tuned the extinction spectra from visible wavelength (silver/gold nanoparticles with diameter of 10 nm or 5 nm) to near infrared wavelength, which is in the range of evanescent wave (Fig. 4(a)–(c)). The nanospheres were conjugated to the tapered microfiber to form an interface through the electrostatic attraction (Fig. 4(d)). Thus, except the assembling surface area enlargement effect, the nanosphere interface here enhanced the evanescent field by near-infrared plasmonic electromagnetic field enhancement [42].

The sensor with raspberry-like nanosphere interface presented highly enhanced detection performance as shown in Fig. 5 [42]. The sensitivity (with Sieve@Ag-10) was twice of that of the sensor with only SiO₂ nanospheres (no plasmonic effect), with LOD of 1.65×10^{-15} M which is three-order higher than non-decorated molecular sieve. This phenomenon proved that the sensitivity amplification effect of the raspberry-like nanosphere interface was not only due to the assembling surface area enlargement.

We compared the electromagnetic field enhancement effects of silver and gold nanoparticles with different diameters (5 nm or 10 nm)-coating nanosphere as shown in Table I [42], and found

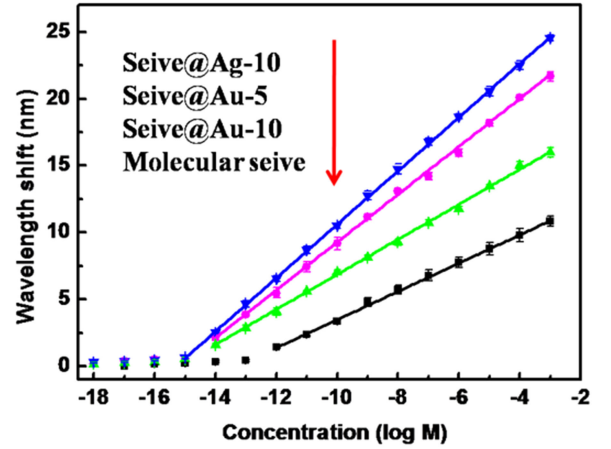


Fig. 5. Experimental transmission wavelength shift of the nanosphere-functionalized sensors. The concentrations of solution are in the range from 10^{-18} to 10^{-3} M. (Sieve@Ag-10: SiO₂ nanosphere with silver nanoparticle with 10 nm-diameter as outer coating; Sieve@Au-5: SiO₂ nanosphere with gold nanoparticle with 5 nm-diameter as outer coating; Sieve@Au-10: SiO₂ nanosphere with gold nanoparticle with 10 nm-diameter as outer coating; Molecular sieve: SiO₂ nanosphere without novel metal nanoparticles.).

TABLE I
SENSITIVITY ENHANCEMENT AND LOD OF MICROFIBER SENSOR AND THE ELECTRIC FIELD ENHANCEMENT RATIO OF INDIVIDUAL NANOSPHERES

Microfiber with interfaces	Individual nanosphere electric field enhancement ratio	Sensitivity (nm/log M)	LOD (M)
Molecular sieve	1	1.0	3.11×10^{-12}
Sieve@Au-10	1.7	1.3	2.51×10^{-14}
Sieve@Au-5	1.9	1.8	1.84×10^{-14}
Sieve@Ag-10	2.6	2.0	1.65×10^{-15}

the improvement of sensor sensitivity and LOD is highly relative to the electric field enhancement of nanospheres. The interface composed with silver nanoparticle-coating nanosphere possessed higher electromagnetic field enhancement (~ 2.6 times) than that without electromagnetic field enhancement, and also higher than the gold nanoparticle-coating nanosphere. The sensor response to biomolecular binding can be expressed by [43]

$$\Delta\lambda = \frac{\alpha_{ex}\sigma_p |E(x,y)|^2 \Delta\beta}{2\varepsilon_s \Gamma} \quad (1)$$

where α_{ex} represents excessive polarizability induced by a single bound molecule, σ_p denotes biomolecular surface density, ε_s is the relative permittivity, $\Delta\beta$ represents the difference in propagation constant between the two optical modes, $\Gamma = \frac{\delta(\Delta\beta)}{\delta\lambda}$ is the dispersion factor which is determined by the refractive index and geometry of the microfiber. Notably, the sensitivity of microfiber sensor is proportional to the surface intensity density $|E(x,y)|^2$. The slight interface energy enhancement could induce a large improvement of LOD. Thus, the improved LOD of this sensor dues to the interface electric field enhancement of plasmonic effect. This sensor could fully afford the measurement of ultralow GABA concentration fluctuations down to 10^{-12} M [44].

It is worth noting that the raspberry-like nanospheres here could also provide a substrate for immunoassay. For

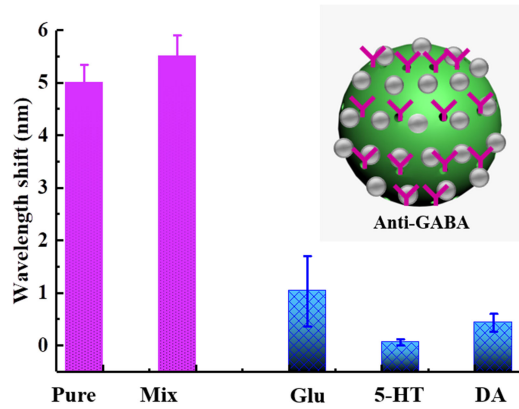


Fig. 6. Comparison of optical response of the sensor functionalized by anti-GABA modified nanospheres (Concentrations: GABA: 10^{-12} M; glucose: 10^{-3} M; serotonin (5-HT): 10^{-6} M; dopamine (DA): 10^{-6} M; mixture: including of all these contents.).

immunoassay GABA sensor, the GABA antibody (anti-GABA) molecules were employed as recognition elements. The anti-GABA molecules were anchored on the raspberry-like nanosphere surface as shown in Fig. 6 [42]. Then, the nanospheres were functionalized on the silica microfiber surface. The sensor presented a predominant optical response to ultralow concentration-GABA molecules (10^{-12} M), while no obvious response was shown to the high-concentration interfering molecules (glucose with 10^{-3} M) and other neurotransmitters with similar sizes (serotonin (5-HT) and dopamine (DA) with 10^{-6} M). The more important is, this biosensor can recognize the GABA molecules with ultralow concentration in the presence of high-concentration interfering molecules. In this case, the incorporation of nanospheres and fiber-optic interferometer improved the GABA concentration sensitivity of sensor from two aspects: Firstly, increasing the assembling surface area: the large surface area of nanospheres improved the ability of assembling recognition elements and catching target molecules. Secondly, enhancing the evanescent field energy density through near-infrared plasmonic electromagnetic field enhancement. The inherent advantages of this sensor (e.g., ultrahigh sensitivity, improved LOD, and small size) provided a potential to fully incorporation into various biomedical applications.

IV. INTERFACE SENSITIZED CELLULAR CYTOCHROME C SENSOR

As a multi-functional enzyme, cytochrome c is involved in both life and death decisions of cells [45]. Its release from mitochondria is an essential signal of the initial progression of programmed cell death [46]. Therefore, in clinical disease diagnosis, the monitoring of cytochrome c, which serves as an apoptosis biomarker, is of great importance to understand certain diseases at the cellular level [47], [48]. However, the lowest LOD of the techniques available currently in laboratories to measure cytochrome c is only 10^{-12} M [46], which is insufficient to trace the initiation of apoptosis in situ (out of cells). It is important and challenging to develop cytochrome c sensor with improved LOD.

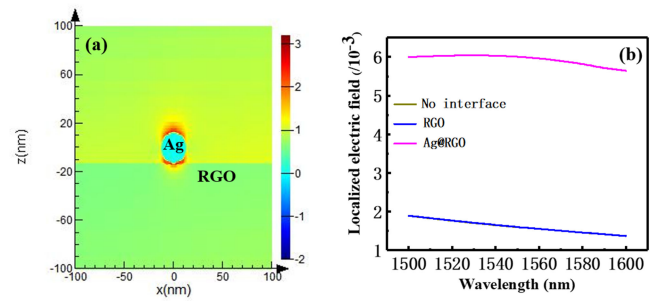


Fig. 7. (a) The calculated near-field intensity mapping of the microfiber interface functionalized by Ag@RGO. (b) The localized electric field of the different nanointerfaces (Ag@RGO, reduced graphene oxide (RGO) and without any interface) over a near-infrared wavelength range of 1500–1600 nm.

We have developed ultrasensitive cytochrome c sensor based on microfiber mode interferometer and interface sensitization strategy. A silver-decorated graphene (Ag@RGO) nanointerface was constructed on optical microfiber surface, and to assembling aptamer layer [49]. The silver nanoparticles were chemically bonded with the RGO nanosheets [50]. The silica microfiber surface was modified by sequential with piranha solution and APTES solution, to produce positive charge [33]. The nanointerface was functionalized onto the silica microfiber surface by the electrostatic attraction between the amino groups on microfiber and the remaining oxygen containing groups on RGO nanosheets [51]. This sensor with high sensitivity was employed for real-time cellular cytochrome c monitoring. The improvement of sensitivity was due to the comprehensive contribution of nanointerface:

- i) Surface evanescent field of microfiber was enhanced by the localized electric field of silver nanoparticles, which made the sensor more sensitive to the target molecule capture-induced RI change;
- ii) On the other hand, the reduced graphene oxide (RGO) platform also contributed to the improvement in sensing performance through providing higher effective contact area and more binding sites (that is, assembling surface area increasing) as well as coupling with the electromagnetic field of silver nanoparticles.

Fig. 7(a) [49] visually presents the near-field intensity distribution on the surface of Ag@RGO nanointerface-functionalized microfiber, while Fig. 7(b) [49] shows that the electric field enhancement of the Ag@RGO-functionalized microfiber at ~ 1560 nm was approximately 4 times higher than that of the microfiber without any interface. Therefore, the as-prepared sensor displayed much better detection capability versus cytochrome c than that without interface functionalization (Fig. 8 [49]). The sensitivity of sensor with Ag@RGO interface was 4 times higher than that of the sensor without interface. More exciting, the LOD was nine orders of magnitude lower compared to that without interface as shown in Table II [49].

It is worth noting that, as a sensor in control experiment, microfiber with graphene oxide (GO, within 5 layers) nanointerface (Fig. 8(b)) [49] also presented an increased sensitivity compared to the sensor without interface (Fig. 8(c)) [49]. The corresponding LOD was nearly six orders of magnitude lower.

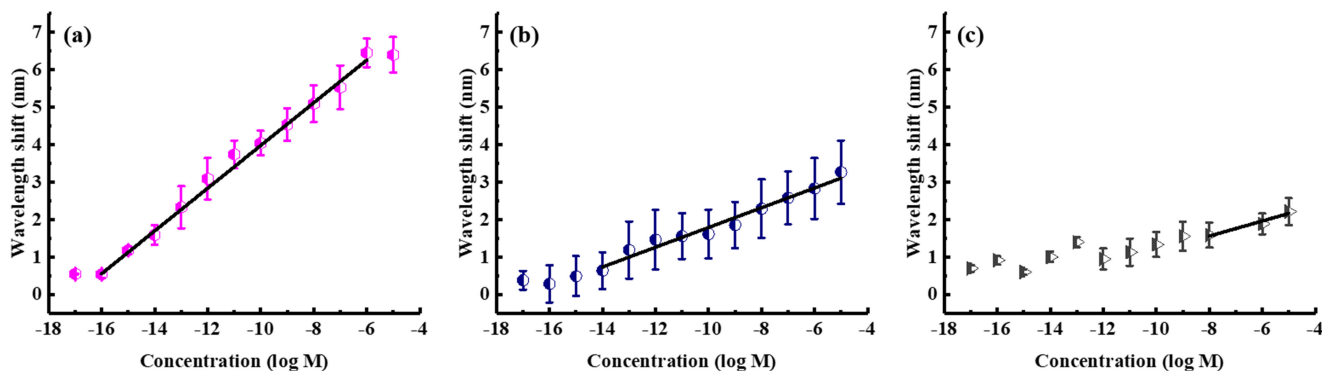


Fig. 8. The wavelength shifts of the sensor with various nanointerfaces versus the concentrations of cytochrome c. (a) Sensor with Ag@RGO nanointerface. (b) Sensor with GO nanointerface. (c) Sensor without any interface.

TABLE II
SENSING ABILITIES OF THE AG@RGO-FUNCTIONALIZED OPTICAL MICROFIBER AND CONTROL SENSORS

Interfaces	Sensitivity/(nm/log M)	LOD/M
Ag@RGO	0.583	6.82×10^{-17}
GO	0.265	2.40×10^{-14}
None	0.160	1.88×10^{-8}

In this case, the GO nanointerface, as a kind of membrane mentioned in Section III, improved the sensitivity through the assembling surface area increasing; providing high surface area [52] and more binding sites [53]. It led to increased quantity and stability of biorecognition molecules immobilized versus the naked silica fiber without interface. This effect has been mentioned in Section III.

Finally, the microfiber with Ag@RGO nanointerface was employed in a real-time cellular cytochrome c monitoring. Its ultralow LOD of 6.82×10^{-17} M enabled the in-situ detection of the ultralow concentrations of cytochrome c present during the initial stage of apoptosis.

V. CONCLUSION

We have reported the progress of our recent development on ultrasensitive optical microfiber biosensors based on interfacial modification and functionalization. The sensitivity and LOD can be significantly improved by enlarging the assembling interface area to assemble more biorecognition elements and by enhancing the energy density of the evanescent field to enhance the light-matter interaction. The assembling interface area was enlarged by immobilize silica micro/nano-sphere arrays onto the microfiber surface. To enhance the energy density of the evanescent field, silver or gold nanoparticles were employed to cover on the micro/nano-sphere surface. With the above sensitization strategies, ultrasensitive microfiber biosensors for γ -amino-butyric acid (GABA) and cellular cytochrome c with LOD of 1.65×10^{-15} M and 6.82×10^{-17} M, respectively were realized. Although in our works, microfiber mode interferometers were employed as RI transducers, the interfa-

cial sensitization strategies demonstrated here are applicable to other fiber optic RI transducers.

REFERENCES

- [1] N. Chaniotakis and N. Sofikiti, "Novel semiconductor materials for the development of chemical sensors and biosensors: A review," *Analytica Chimica Acta*, vol. 615, pp. 1–9, 2008.
- [2] M. Pospisilova, C. Kuncova, and J. Trogl, "Fiber-optic chemical sensors and fiber-optic bio-sensors," *Sensors*, vol. 15, pp. 25208–25259, 2015.
- [3] X. Fan, I. M. White, S. I. Sphopova, H. Zhu, J. D. Suter, and Y. Sun, "Sensitive optical biosensors for unlabeled targets: A review," *Analytica Chimica Acta*, vol. 620, pp. 8–26, 2008.
- [4] M. I. J. Stich, L. H. Fisher, and O. S. Wolfbeis, "Multiple fluorescent chemical sensing and imaging," *Chem. Soc. Rev.*, vol. 39, pp. 3102–3114, 2010.
- [5] T. Lin, Y. Lu, and C. Hsu, "Fabrication of glucose fiber sensor based on immobilized GOD technique for rapid measurement," *Opt. Express*, vol. 18, no. 26, pp. 27560–27566, 2010.
- [6] X. Liu, Y. Qin, C. Deng, J. Xiang, and Y. Li, "A simple and sensitive impedimetric aptasensor for the detection of tumor markers based on gold nanoparticles signal amplification," *Talanta*, vol. 132, pp. 150–154, 2015.
- [7] S. Bidmanova, R. Chaloupkova, J. Damborsky, and Z. Prokop, "Development of an enzymatic fiber-optic biosensor for detection of halogenated hydrocarbons," *Anal. Bioanal. Chem.* vol. 398, pp. 1891–1898, 2010.
- [8] C. Wu *et al.*, "A nonenzymatic hairpin DNA cascade reaction provides high signal gain of mRNA imaging inside live cells," *J. Amer. Chem. Soc.*, vol. 137, pp. 4900–4903, 2015.
- [9] A. M. Shrivastav, S. K. Mishra, and B. D. Gupta, "Fiber optic SPR sensor for the detection of melamine using molecular imprinting," *Sensors Actuators B, Chem.*, vol. 212, pp. 404–410, 2015.
- [10] J. Guo *et al.*, "Highly stretchable, strain sensing hydrogel optical fibers," *Adv. Mater.*, vol. 28, pp. 10244–10249, 2016.
- [11] S. K. Mishra, S. N. Tripathi, V. Choudhary, and B. D. Gupta, "SPR based fibre optic ammonia gas sensor utilizing nanocomposite film of PMMA/reduced graphene oxide prepared by in situ polymerization," *Sensors Actuators B, Chem.*, vol. 199, pp. 190–200, 2014.
- [12] A. Leung, P. M. Shankar, and R. Mutharasan, "Label-free detection of DNA hybridization using gold-coated tapered fiber optic biosensors (TFOBS) in a flow cell at 1310 nm and 1550 nm," *Sensors Actuators B, Chem.*, vol. 131, pp. 640–645, 2008.
- [13] G. Quero *et al.*, "Long period fiber grating nano-optrode for cancer biomarker detection," *Biosensors Bioelectron.*, vol. 80, pp. 590–600, 2016.
- [14] F. Chiavaioli *et al.*, "Towards sensitive label-free immunosensing by means of turn-around point long period fiber gratings," *Biosensors Bioelectron.*, vol. 60, pp. 305–310, 2014.
- [15] A. Deep *et al.*, "Immobilization of enzyme on long period grating fibers for sensitive glucose detection," *Biosensors Bioelectron.*, vol. 33, pp. 190–195, 2012.
- [16] A. N. Chryssis, S. S. Saini, S. M. Lee, H. Yi, W. E. Bentley, and M. Dagenais, "Detecting hybridization of DNA by highly sensitive evanescent field etched core fiber Bragg grating sensors," *IEEE J. Sel. Topics Quantum Electron.*, vol. 11, no. 4, pp. 864–872, Jul./Aug. 2005.

- [17] D. D. Sun, T. Guo, and B. O. Guan, "Label-free detection of DNA hybridization using a reflective microfiber Bragg grating biosensor with self-assembly technique," *J. Lightw. Technol.*, vol. 35, no. 16, pp. 3354–3359, Aug. 2017.
- [18] D. Sun, T. Guo, Y. Ran, Y. Huang, and B.-O. Guan, "In-situ DNA hybridization detection with a reflective microfiber grating biosensor," *Biosensors Bioelectron.*, vol. 61, pp. 541–546, 2014.
- [19] L. Han *et al.*, "Specific detection of aquaporin-2 using plasmonic tilted fiber grating sensors," *J. Lightw. Technol.*, vol. 35, no. 16, pp. 3360–3365, Aug. 2017.
- [20] T. Guo *et al.*, "Highly sensitive detection of urinary protein variations using tilted fiber grating sensors with plasmonic nanocoatings," *Biosensors Bioelectron.*, vol. 78, pp. 221–228, 2016.
- [21] S. Maguis *et al.*, "Biofunctionalized tilted fiber Bragg gratings for label-free immunosensing," *Opt. Express*, vol. 16, pp. 19049–19062, 2008.
- [22] K. E. You, N. Uddin, T. H. Kim, Q. H. Fan, and H. D. Yoon, "Highly sensitive detection of biological substances using microfluidic enhanced Fabry-Perot etalon-based optical biosensors," *Sensors Actuators B, Chem.*, vol. 277, pp. 62–68, 2018.
- [23] M. I. Zibaii *et al.*, "Label free fiber optic aptamer-biosensor for in-vitro detection of dopamine," *J. Lightw. Technol.*, vol. 34, no. 19, pp. 4516–4524, Oct. 2016.
- [24] L. H. Chen *et al.*, "Label-free fiber-optic interferometric immunosensors based on waist-enlarged fusion taper," *Sensors Actuators B, Chem.*, vol. 178, pp. 176–184, 2013.
- [25] B. Song, H. Zhang, B. Liu, W. Lin, and J. Wu, "Label-free in-situ real-time DNA hybridization kinetics detection employing microfiber-assisted Mach-Zehnder interferometer," *Biosensors Bioelectron.*, vol. 81, pp. 151–158, 2016.
- [26] M. J. Yin *et al.*, "Label-free, disposable fiber-optic biosensors for DNA hybridization detection," *Analyst*, vol. 138, pp. 1988–1994, 2013.
- [27] W. Yu, T. Lang, J. Bian, and W. Kong, "Label-free fiber optic biosensor based on thin-core modal interferometer," *Sensors Actuators B, Chem.*, vol. 228, pp. 322–329, 2016.
- [28] Y. Y. Huang *et al.*, "High-sensitivity DNA biosensor based on optical fiber taper interferometer coated with conjugated polymer tentacle," *Opt. Express*, vol. 23, pp. 26962–26968, 2015.
- [29] B. Yu, Y. Y. Huang, J. Zhou, T. Guo, and B.-O. Guan, "Understanding the pH-dependent interaction between graphene oxide and single-stranded DNA through a fiber-optic interferometer," *Phys. Chem. Chem. Phys.*, vol. 18, pp. 32266–32271, 2016.
- [30] M. R. Bennett, and V. J. Balcar, "Forty years of amino acid transmission in the brain," *Neurochem. Int.*, vol. 35, pp. 269–280, 1999.
- [31] L. M. Levy, and A. J. Degnan, "GABA-based evaluation of neurologic conditions: MR spectroscopy," *Amer. J. Neuroradiol.*, vol. 34, pp. 259–265, 2013.
- [32] K. Li, G. Liu, Y. Wu, P. Hao, W. Zhou, and Z. Zhang, "Gold nanoparticle amplified optical microfiber evanescent wave absorption biosensor for cancer biomarker detection in serum," *Talanta*, vol. 120, pp. 419–424, 2014.
- [33] R. M. Pasternack, S. R. Amy, and Y. J. Chabal, "Attachment of 3-(aminopropyl) triethoxysilane on silicon oxide surfaces: Dependence on solution temperature," *Langmuir*, vol. 24, pp. 12963–12971, 2008.
- [34] Y. Huang *et al.*, "Ultrasensitive and label-free detection of γ -aminobutyric acid using fiber-optic interferometric sensors functionalized with size-selective molecular sieve arrays," *Sensors Actuators B, Chem.*, vol. 244, pp. 934–940, 2017.
- [35] M. F. Ding, Y. Y. Huang, T. Guo, L. P. Sun, and B.-O. Guan, "Mesoporous nanospheres functionalized optical microfiber biosensor for low concentration neurotransmitter detection," *Opt. Express*, vol. 24, pp. 27152–27159, 2016.
- [36] K. Mun, S. D. Alvarez, W. Choi and M. J. Sailor, "A stable, label-free optical interferometric biosensor based on TiO₂ nanotube arrays," *ACS Nano*, vol. 4, no. 4, pp. 2070–2076, 2010.
- [37] J. A. Lee, K. C. Krogman, M. Ma, R. M. Hill, P. T. Hammond, and G. C. Rutledge, "Highly reactive multilayer-assembled TiO₂ coating on electrospun polymer nanofibers," *Adv. Mater.*, vol. 21, pp. 1252–1256, 2009.
- [38] H. S. Shin, Y. S. Jang, Y. Lee, Y. Jung, S. B. Kim, and H. C. Choi, "Photoinduced self-assembly of TiO₂ and SiO₂ nanoparticles on sidewalls of single-walled carbon nanotube," *Adv. Mater.*, vol. 19, pp. 2873–2876, 2007.
- [39] A. Bialiaieu, A. Bottomley, D. Prezgot, A. Ianoul, and J. Albert, "Plasmon-enhanced refractometry using silver nanowire coatings on tilted fibre Bragg gratings," *Nanotechnology*, vol. 23, no. 44, 2012, Art. no. 4012.
- [40] J. Renoirt, M. Debliquy, J. Albert, A. Ianoul, and C. Caucheteur, "Surface plasmon resonances in oriented silver nanowire coatings on optical fibers," *J. Phys. Chem. C*, vol. 118, no. 20, pp. 11035–11042, 2014.
- [41] S. Lepinay, A. Staff, A. Ianoul, and J. Albert, "Improved detection limits of protein optical fiber biosensors coated with gold nanoparticles," *Biosensors Bioelectron.*, vol. 52, pp. 337–344, 2014.
- [42] Y. Huang *et al.*, "A fiber-optic sensor for neurotransmitters with ultralow concentration: Near-infrared plasmonic electromagnetic field enhancement using raspberry-like meso-SiO₂ nanospheres," *Nanoscale*, vol. 9, pp. 14929–14936, 2017.
- [43] L. Liang, L. Jin, Y. Ran, L. Sun, and B. Guan, "Interferometric detection of microRNAs using a capillary optofluidic sensor," *Sensors Actuators B, Chem.*, vol. 242, pp. 999–1006, 2017.
- [44] C. N. Epperson *et al.*, "Cortical γ -aminobutyric acid levels across the menstrual cycle in healthy women and those with premenstrual dysphoric disorder," *Arch. Gen. Psychiatry*, vol. 59, pp. 851–858, 2002.
- [45] C. Fan, K. W. Plasco, and A. J. Heeger, "High-efficiency fluorescence quenching of conjugated polymers by proteins," *J. Amer. Chem. Soc.*, vol. 124, pp. 5642–5643, 2002.
- [46] P. Manickam, A. Kaushik, C. Karunakaran, and S. Bhansali, "Recent advances in cytochrome c biosensing technologies," *Biosens. Bioelectron.*, vol. 87, pp. 654–668, 2017.
- [47] S. Peng *et al.*, "Sequentially programmable and cellularly selective assembly of fluorescent polymerized vesicles for monitoring cell apoptosis," *Adv. Sci.*, vol. 4, 2017, Art. no. 1700310.
- [48] M. Cao, C. Cao, M. Liu, P. Wang, and C. Zhu, "Selective fluorometry of cytochrome c using glutathione-capped CdTe quantum dots in weakly basic medium," *Microchimica Acta*, vol. 165, pp. 341–346, 2009.
- [49] H. Li *et al.*, "Real-time cellular cytochrome c monitoring through an optical microfiber: Enabled by a silver-decorated graphene nanointerface," *Adv. Sci.*, vol. 5, 2018, Art. no. 1701704.
- [50] H. Tien *et al.*, "Using self-assembly to prepare a graphene-silver nanowire hybrid film that is transparent and electrically conductive," *Carbon*, vol. 58, pp. 198–207, 2013.
- [51] K. Shi *et al.*, "Near-infrared light-responsive poly(N-isopropylacrylamide)/graphene oxide nanocomposite hydrogels with ultrahigh tensibility," *ACS Appl. Mater. Interfaces*, vol. 7, pp. 27289–27298, 2015.
- [52] J. A. Mann, T. Alava, H. G. Craighead, and W. R. Dichtel, "Preservation of antibody selectivity on graphene by conjugation to a tripod monolayer," *Angewandte Chemie Int. Ed.*, vol. 125, pp. 3259–3262, 2013.
- [53] R. K. Srivastava *et al.*, "Functionalized multilayered graphene platform for urea sensor," *ACS Nano*, vol. 6, pp. 168–175, 2012.